PNAS RESEARCH ARTICLE | CELL BIOLOGY

ABL kinases regulate the stabilization of HIF-1α and MYC through CPSF1

Benjamin Mayro[a], Jacob P. Hoj[a], Christian G. Cerda-Smith[a], Haley M. Hutchinson[a], Michael W. Caminear[a], Hannah L. Thrash[a], Peter S. Winter[a], Suzanne E. Wardell[a], Donald P. McDonnell[a,b], Colleen Wu[c], Kris C. Wood[a,b], and Ann Marie Pendergast[a,b,1]

Edited by Stephen Goff, Columbia University Irving Medical Center, New York, NY; received June 16, 2022; accepted February 7, 2023

The hypoxia-inducible factor 1-α (HIF-1α) enables cells to adapt and respond to hypoxia (Hx), and the activity of this transcription factor is regulated by several oncogenic signals and cellular stressors. While the pathways controlling normoxic degradation of HIF-1α are well understood, the mechanisms supporting the sustained stabilization and activity of HIF-1α under Hx are less clear. We report that ABL kinase activity protects HIF-1α from proteasomal degradation during Hx. Using a fluorescence-activated cell sorting (FACS)-based CRISPR/Cas9 screen, we identified HIF-1α as a substrate of the cleavage and polyadenylation specificity factor-1 (CPSF1), an E3-ligase which targets HIF-1α for degradation in the presence of an ABL kinase inhibitor in Hx. We show that ABL kinases phosphorylate and interact with CUL4A, a cullin ring ligase adaptor, and compete with CPSF1 for CUL4A binding, leading to increased HIF-1α protein levels. Further, we identified the MYC proto-oncogene protein as a second CPSF1 substrate and show that active ABL kinase protects MYC from CPSF1-mediated degradation. These studies uncover a role for CPSF1 in cancer pathobiology as an E3-ligase antagonizing the expression of the oncogenic transcription factors, HIF-1α and MYC.

ABL kinases | HIF-1α | MYC | CPSF1 | E3-ligase

Oxygen is essential for the survival of all aerobic organisms. As a result, pathways have evolved to allow cells to sense and respond to fluctuations in oxygen availability. In the presence of oxygen, hypoxia-inducible factor-α (HIF-α) is prolyl-hydroxylated by a family of 2-oxoglutarate-dependent dioxygenases (PHD1-3) and, subsequently, interacts with the von Hippel–Lindau ubiquitin ligase (pVHL) complex (1–7). This complex ubiquitinates HIF-α, promoting its degradation by the 26*S* proteasome under normoxia (Nx). In hypoxic cellular environments, VHL does not interact with HIF-α, resulting in its accumulation in cells (4). Stabilized HIF-α dimerizes with constitutively expressed HIF-1β to form an active HIF transcriptional complex that controls the expression of target genes needed for adaptation to hypoxic environments (1, 2, 4).

The mechanism(s) regulating the degradation of HIF-α during Nx by the pVHL complex are well understood. However, the signaling pathways and factors that support the sustained expression and activation of HIF-α during Hx outside of PHD inhibition are not as clearly defined (8). We and others have shown that the ABL family of nonreceptor tyrosine kinases, ABL1 and ABL2, enable cancer cells to respond to diverse stress stimuli by activating pathways necessary for survival (9–12). The ABL kinases often potentiate these responses by inducing the stability and/or transactivation of transcriptional regulators (9, 12–16). Thus, we hypothesized that the ABL kinases may modulate the cellular response to Hx. We found that ABL kinase activity is necessary for the stabilization of Hx-inducible factor 1-α (HIF-1α) protein during Hx, and activation of the ABL kinases during Nx was sufficient to elevate HIF-1α protein levels. Further, we show that the ABL kinases promote HIF-1α protein stability in Hx by protecting it from proteasomal degradation. Using a flow cytometry-based CRISPR/Cas9 screen, we identified cleavage and polyadenylation specificity factor-1 (CPSF1) as the E3-ligase targeting HIF-1α for destruction after ABL kinase inhibition. Notably, we determined that a second oncoprotein transcription factor, MYC, is also regulated by the ABL–CPSF1 axis. These data reveal a critical role for the ABL kinases in supporting the stabilization of the oncogenic transcription factors HIF-1α and MYC by antagonizing the activity of the CPSF1 E3-ligase complex.

Results

ABL Kinase Inhibition Decreases HIF-1α Protein Levels in Hx. Pharmacological inhibition of the ABL kinases using the allosteric inhibitors ABL001 or GNF5 decreased HIF transcriptional activity as assessed using a Hx response element reporter stably expressed in either EGFR-mutant PC9 lung cancer cells or in HEK293T cells under hypoxic

Significance

The hijacking of transcription factor networks to drive processes of pathological importance is a common occurrence in cancer. Hypoxia-inducible factor 1-α (HIF-1α) and MYC are transcription factors that induce the expression of genes essential for cancer progression. Here, we report that HIF-1α and MYC are both indirectly targetable through inhibition of ABL kinases. Mechanistically, we found that loss of ABL kinase activity leads to the recognition and subsequent ubiquitination of HIF-1α and MYC by the cleavage and polyadenylation specificity factor-1 (CPSF1) E3-ligase complex leading to their proteasomal degradation.

Author contributions: B.M., J.P.H., C.G.C.-S., and A.M.P. designed research; B.M., J.P.H., C.G.C.-S., H.M.H., M.W.C., and H.L.T. performed research; P.S.W. and S.E.W. contributed new reagents/analytic tools; B.M., J.P.H., and C.G.C.-S. analyzed data; B.M. conceptualization, methodology, investigation, visualization, funding acquisition, project administration; J.P.H. and C.G.C.-S. methodology, investigation, visualization, funding acquisition, writing–review & editing; H.M.H. and M.W.C. investigation, writing–review & editing; P.S.W. and S.E.W. methodology, writing–review & editing; D.P.M. funding acquisition, supervision; C.W. supervision; K.C.W. funding acquisition, supervision, writing–review & editing; and B.M., D.P.M., C.W., K.C.W., and A.M.P. wrote the paper.

Competing interest statement: A.M.P. is a consultant and advisory board member for The Pew Charitable Trusts. All other authors declare that they have no competing interests.

This article is a PNAS Direct Submission.

[1]To whom correspondence may be addressed. Email: ann.pendergast@duke.edu.

This article contains supporting information online at https://www.pnas.org/lookup/suppl/doi:10.1073/pnas.2210418120/-/DCSupplemental.

Published April 11, 2023.

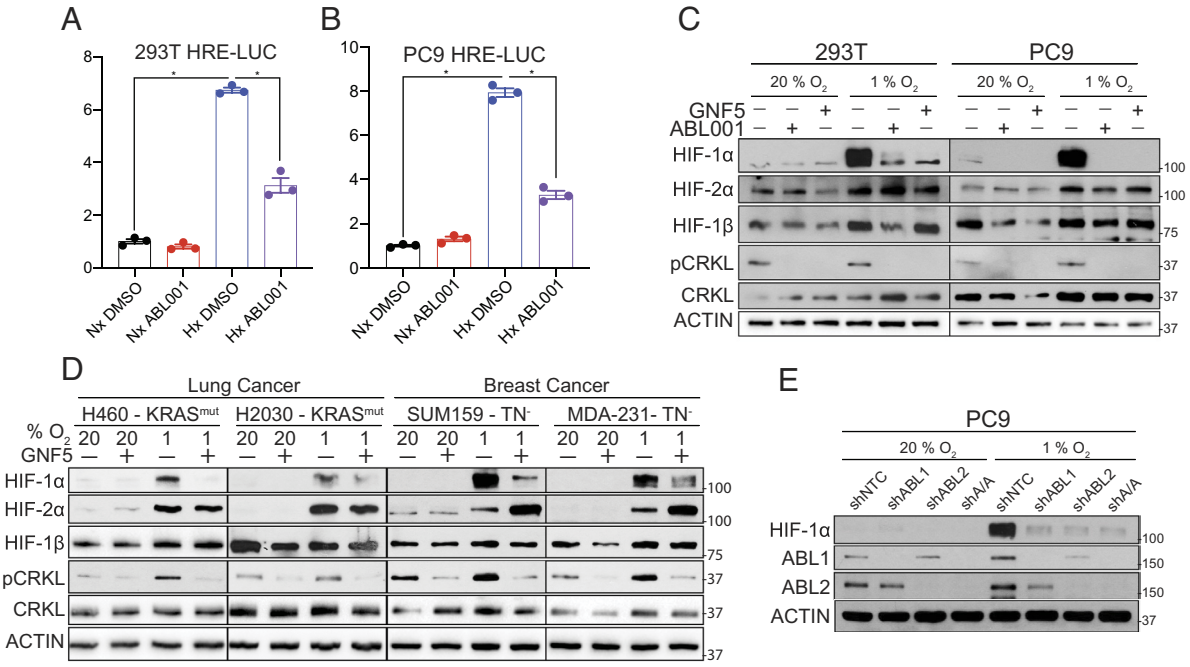

Fig. 1. ABL kinases are necessary for hypoxic accumulation of HIF-1α. (*A* and *B*) Bioluminescence levels of PC9 and 293T cells transduced with a hypoxia response element reporter and treated with ABL001 (20 μM) during normoxia (Nx) or hypoxia (Hx) (1% O_2) for 24 h. (*C*) Immunoblot (IB) analysis of whole-cell lysates (WCL) derived from HEK293T and PC9 cells treated with ABL001 (20 μM) or GNF5 (20 μM) during normoxia or hypoxia (1% O_2) for 24 h. (*D*) IB analysis of WCL derived from KRAS-mutant lung cancer cells (H460, H2030) and triple-negative (TN−) breast cancer cells (SUM159, MDA-MB-231) treated with GNF5 during normoxia or hypoxia (1% O_2) for 24 h. (*E*) IB analysis of WCL derived from PC9 cells transduced with indicated short hairpin RNA (shRNA) lentiviruses and cultured under normoxia or hypoxia for 24 h.

conditions (Fig. 1 *A* and *B* and *SI Appendix* Fig. S1 *A–C*). As the ABL kinases have previously been shown to regulate the expression of transcriptional regulators (9, 12–16), we investigated the extent to which decreased HIF activity observed in hypoxic conditions was attributable to changes in the abundance of the HIF family members, HIF-1α, -2α, and 1β. Treatment with allosteric ABL kinase inhibitors resulted in decreased HIF-1α protein levels in multiple EGFR- or KRAS-mutant lung cancer cells and in triple-negative breast cancer cells without a consistent change in HIF-2α or HIF-1β levels (Fig. 1 *C* and *D*). Treatment with an orthosteric, ATP-competitive ABL kinase inhibitor, nilotinib, elicited a similar decrease in HIF-1α levels without impacting HIF-2α and HIF-1β levels (*SI Appendix* Fig. S2*A*). The maintenance of HIF-1α protein levels during pseudohypoxia (chemically induced Hx) was also dependent on ABL kinase activity (*SI Appendix* Fig. S2*B*). The ABL1 and ABL2 nonreceptor tyrosine kinases have a highly homologous amino terminal kinase domain (90%) and a carboxy terminal domain (29%) that evolutionarily diverged after a gene duplication event (17). We and others have found both overlapping and nonredundant functions for the ABL kinases (12). Knockdown of either ABL1 or ABL2 resulted in a profound decrease in HIF-1α protein levels in hypoxic conditions, suggesting a threshold effect of decreased ABL kinase activity (Fig. 1*E* and *SI Appendix* Fig. S2*C*).

ABL Activation Increases HIF-1α Protein Levels. ABL kinase activity, but not total protein levels, becomes elevated in Hx (Figs. 1 *C* and *D* and 2*A*). Thus, we investigated whether the activation of the ABL kinases was sufficient to increase HIF-1α levels. The ABL kinases can be activated with point mutations that disrupt intramolecular inhibitory interactions or treatment with an allosteric activator (*SI Appendix* Fig. S3*A*). Site-direct mutagenesis of two proline (P) residues located in the ABL SH2-SH1 linker to glutamate (E) leads to a release of the ABL autoinhibited state and increased kinase activity (18). Mutation of a single proline residue to glutamate led to a partial activation, while mutation of both proline residues to glutamate produced maximally activated ABL1 and ABL2 kinases as detected by immunoblotting for phosphotyrosine (p-Y) (Fig. 2*B*). This dose-dependent increase in ABL kinase activity resulted in a dose-dependent increase in HIF-1α levels (Fig. 2 *B* and *C* and *SI Appendix* Fig. S3*B*). Similarly, treatment with an allosteric activator (DPH) of the ABL kinases increased HIF-1α levels (Fig. 2*D*).

The enhanced accumulation of HIF-1α protein levels observed upon coexpression of activated ABL1EE was reversed by ABL allosteric inhibitors (Fig. 2*E*). Further, we found that wild-type (WT) and SH3-domain mutated (P131L) ABL1 induced HIF-1α expression, while the catalytically inactive (K290M) ABL1 did not affect HIF-1α levels (Fig. 2*F*). Mutation of the SH2 domain of ABL1 (R171K), which disrupts the binding to tyrosine-phosphorylated substrates, increased HIF-1α protein levels to a lesser extent than active ABL1 mutants (Fig. 2*F*). These data demonstrate that the ABL kinases are necessary to maintain HIF-1α protein under conditions of Hx and that activation of the ABL kinases is sufficient to increase HIF-1α protein levels.

ABL Kinase Regulation of HIF-1α Does Not Occur Transcriptionally. A complex network of signaling pathways enable the accumulation of HIF-1α in Hx through transcriptional, translational, and posttranslational processes (1, 2, 6–8). To investigate the mechanism(s) by which ABL kinase activity impacts HIF-1α levels, we first examined the impact of these enzymes on *HIF1A* mRNA levels. While *HIF1A* mRNA decreased during Hx as shown previously (19), neither pharmacologic inhibition nor short hairpin RNA (shRNA)-mediated knockdown of the ABL kinases resulted in significant alterations of *HIF1A* mRNA levels (*SI Appendix*, Fig. S4 *A* and *B*). Next, we investigated whether the hypoxic stabilization of HIF-1α produced from an ectopically expressed HIF-1α transgene under the control of a heterologous promoter, was impacted by ABL kinase inhibition. Indeed, similar to endogenous HIF-1α, ABL kinase inhibition resulted in decreased

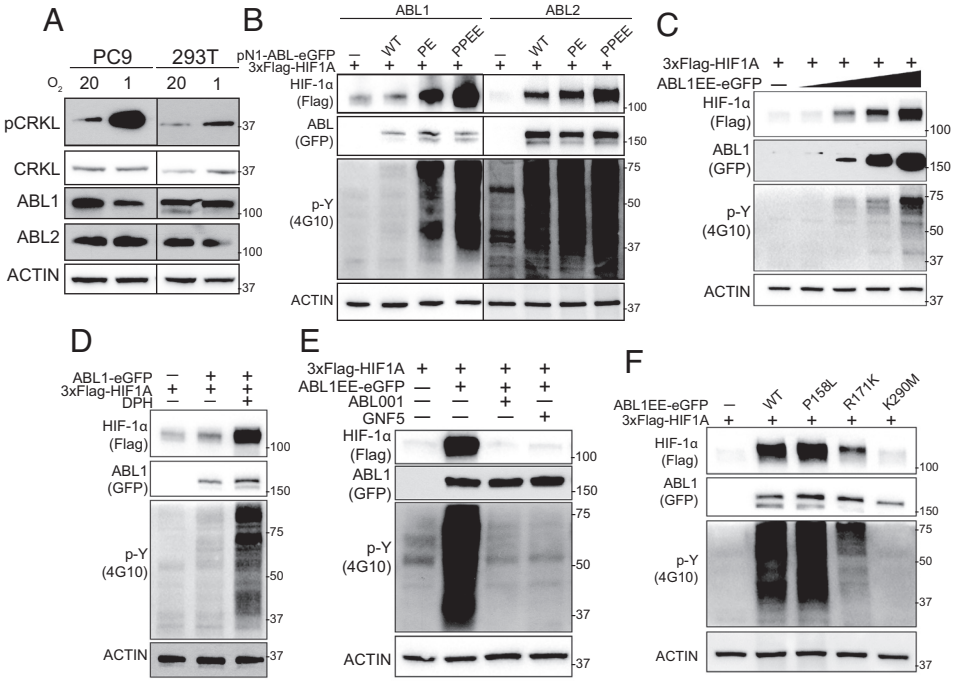

Fig. 2. ABL kinase activation induces HIF-1α protein stabilization. (*A*) IB analysis of WCL derived from PC9 and 293T exposed to normoxia or hypoxia (1% O_2) for 24 h. (*B* and *C*) IB analysis of WCL derived from HEK293T cells transfected with 3xFlag-HIF1A and indicated ABL-eGFP constructs for 48 h. ABL PE has a moderate increase in ABL kinase activity and ABL PPEE elicits a higher increase in ABL kinase activity. (*D*) IB analysis of WCL derived from HEK293T cells transfected with 3xFlag-HIF1A and ABL1-eGFP constructs for 24 h and then treated with the ABL kinase allosteric activator DPH (2.5 μM) as indicated for 24 h before harvesting. (*E*) IB analysis of WCL derived from HEK293T cells transfected with 3xFlag-HIF1A and ABL1-eGFP constructs for 24 h and then treated with ABL001 and GNF5 as indicated for 24 h before harvesting. (*F*) IB analysis of WCL derived from HEK293T cells transfected with 3xFlag-HIF1A and indicated ABL1-eGFP constructs for 48 h.

Flag-HIF-1α protein during Hx (*SI Appendix* Fig. S4*C*). These results suggest that ABL kinase-dependent regulation of HIF-1α may occur posttranslationally.

ABL Kinases Regulate the Proteasomal Degradation of HIF-1α. HIF-1α protein levels are regulated in large part by the activity of the ubiquitin-dependent 26S proteasome pathway (1, 2). We found that decreased expression of endogenous HIF-1α protein induced by ABL allosteric inhibition with GNF5 or upon knockdown of ABL1 and ABL2, was reversed by inhibition of the proteasome with MG132 in lung cancer cells (Fig. 3*A* and *SI Appendix* Fig. S5*A*). Similarly, inhibition of the proteasome with MG132 reversed the decrease of exogenous Flag-tagged-HIF-1α protein levels after ABL kinase inhibition with allosteric inhibitors in HEK293T cells coexpressing kinase-active ABL1EE-eGFP (Fig. 3*B*). Moreover, endogenous HIF-1α was highly ubiquitinated after loss of ABL kinase activity in both lung cancer and breast cancer cells (Fig. 3*C* and *SI Appendix* Fig. S5*B*). Moreover, activation of ABL1 and ABL2 decreased HIF-1α ubiquitination (Fig. 3*D* and *SI Appendix* Fig. S5*C*). Importantly, we found that PC9 and HEK293T cells

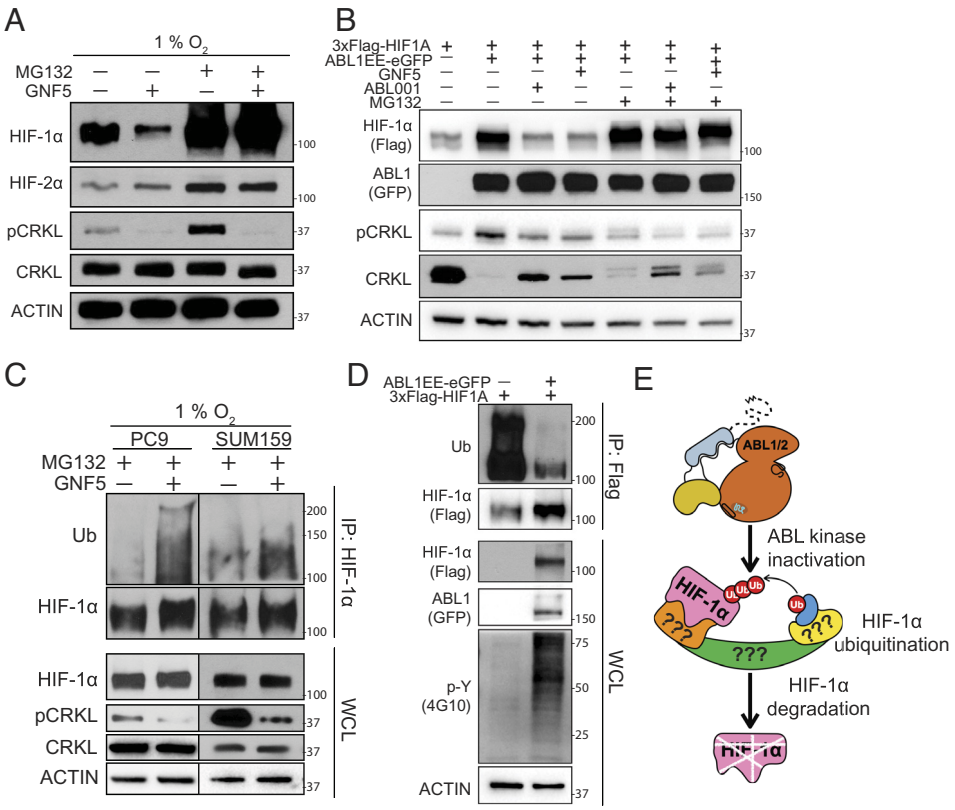

Fig. 3. The ABL kinases regulate the proteasomal degradation of HIF-1α. (*A*) IB analysis of WCL derived from PC9 cells treated with ABL001 and MG132 (4 μM) as indicated during hypoxia for 24 h. (*B*) IB analysis of WCL derived from HEK293T cells transfected with 3xFlag-HIF1A and ABL1-eGFP constructs for 24 h and then treated with ABL001, GNF5, and MG132 as indicated for 24 h before harvesting. (*C*) IB analysis of IP and WCL derived from PC9 and SUM159 cells treated with ABL001 and MG132 as indicated during hypoxia for 24 h. (*D*) IB analysis of IP and WCL derived from HEK293T cells transfected with 3xFlag-HIF1A and ABL1-eGFP constructs for 24 h. (*E*) Proposed model depicting that loss of ABL kinase activity leads to HIF-1α ubiquitination and proteasome-mediated protein degradation.

did not exhibit a global change in total ubiquitination levels and proteasome activity after treatment with the ABL001 allosteric inhibitor (*SI Appendix*, Fig. S6 *A–C*). These data support the model that ABL kinase activity impairs HIF-1α ubiquitination and proteasome-mediated protein degradation without impacting global ubiquitination and proteasome activities (Fig. 3*E*).

Fluorescence-Activated Cell Sorting (FACS)-Based CRISPR/Cas9 Nominates CPSF1 as the ABL-Dependent HIF-1α Targeting E3-Ligase. To identify the ABL-dependent E3-ligase(s) regulating HIF-1α protein stability, we conducted a FACS-based CRISPR/Cas9 screen using a custom sgRNA library targeting 593 known and predicted human E3-ligases in PC9 lung cancer cells. This library was transduced into PC9 cells and then incubated in the presence of an ABL kinase inhibitor in hypoxic conditions for 24 h (Fig. 4*A*). Staining with a fluorophore-conjugated antibody against HIF-1α and subsequent FACS-based sorting of HIF-1α high- and low-expressing cell populations, revealed E3-ligase components that impacted HIF-1α protein levels after ABL inhibition (Fig. 4*B* and *SI Appendix*, Fig. S7 *A–D*). The top scoring genes whose loss rescued HIF-1α protein levels during ABL inhibition included RBX1 and CPSF1, while VHL did not score as a hit (Fig. 4*B* and *SI Appendix*, Fig. S7 *E–G*). RBX1 is a well-studied component of the catalytic core in the majority of multisubunit cullin ring ligase (CRLs) complexes (~500 complexes) (20). Thus, we evaluated how CPSF1 protein might be involved in the regulation of HIF-1α stability.

CPSF1 Is an E3-Ligase Targeting HIF-1α. CPSF1 is an essential gene whose primary known function is as a core scaffolding component of the CPSF complex (21). This complex is necessary for proper 3′-polyadenylation of eukaryotic pre-mRNAs, and loss of CPSF1 impairs the maturation of the bulk of eukaryotic mRNA transcripts (22). In addition to its role in mRNA maturation, CPSF1 shares significant structural similarity with the CRL adaptor DDB1 (23). However, an E3-ligase activity has not previously been ascribed to CPSF1, although it was reported that immunoprecipitated CPSF1 protein complexes from cultured cells exhibit in vitro E3-ligase activity (23, 24). Mining the BioGRID database uncovered CPSF1 as a potential HIF-1α interactor (25, 26). We demonstrated that CPSF1 coimmunoprecipitates with HIF-1α in the presence of the proteasome inhibitor MG132 (Fig. 4*C*). Expression of CPSF1 led to a profound loss of HIF-1α protein accumulation in Hx that was reversed by proteasomal inhibition (Fig. 4 *D* and *E* and *SI Appendix* Fig. S8). HIF-1α was highly ubiquitinated following CPSF1 expression in Hx, thereby establishing a link between this E3 ligase, ubiquitination, and the proteasome (Fig. 4 *F* and *G*).

CPSF1 Is an E3-Ligase Targeting the HIF-1α DNA-Binding Domain (DBD). We next mapped the sites/domains within HIF-1α that were required for CPSF1-dependent degradation. It was determined using deletion analysis that a mutant encompassing the basic helix–loop–helix (bHLH) DBD of HIF-1α (AA 1-71) remained responsive to CPSF1-mediated degradation (Fig. 5*A*). Since the structures of full-length CPSF1 and the DBD of HIF-1α are available, we performed in silico docking of the HIF-1α DBD onto CPSF1 using the HDOCK protein–protein docking server. CPSF1 was predicted to interact with the HIF-1α DBD using the equivalent pocket that DDB1 uses to interact with DDB2 (Fig. 5*B*) (23). The CPSF1 paralog DDB1 has been shown to interact with DxR/DxxR/DxxxR motifs in binding partners such as DDB2, and mutation of the D and R residues is often sufficient to break complex formation (27). Thus, we evaluated whether the single DxxR motif in the HIF-1α DBD might mediate the HIF-1α–CPSF1 interaction. Indeed, mutation of D24 and R27 to alanine

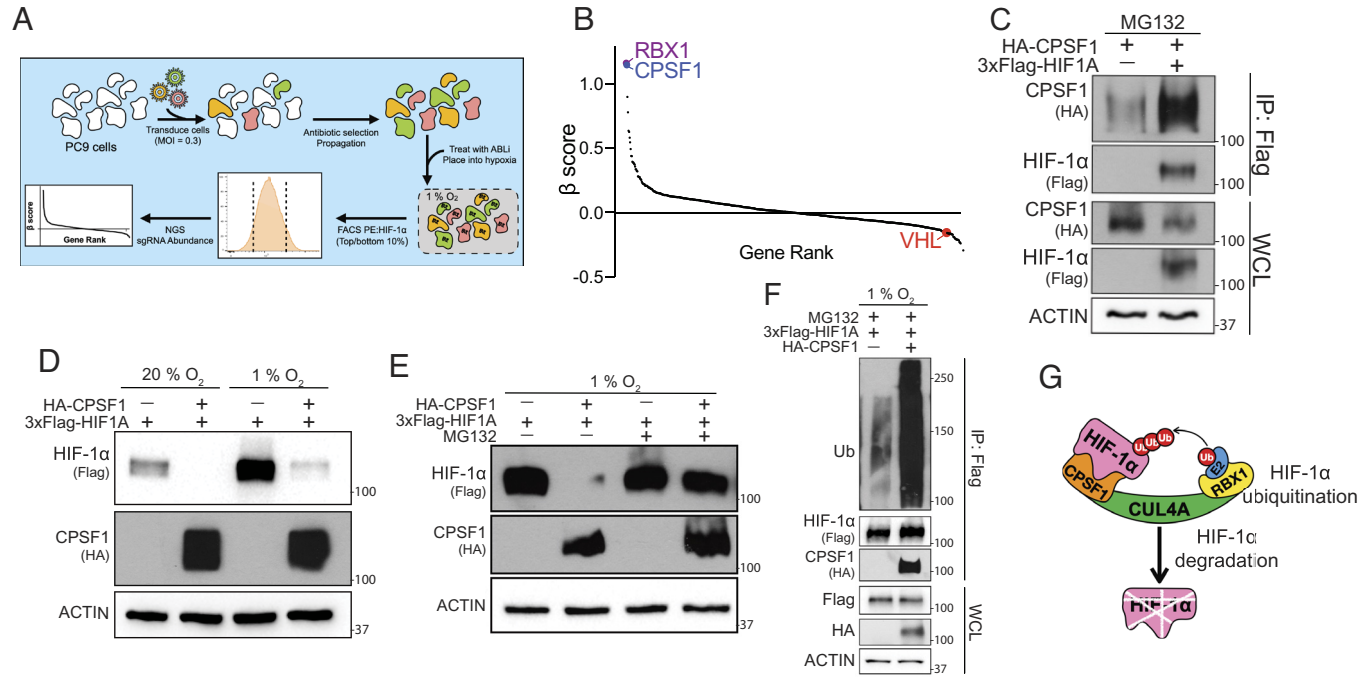

Fig. 4. CPSF1 is a HIF-1α-targeting E3-ligase. (*A*) Scheme of the FACS-based CRISPR E3 ligase screen performed. (*B*) Snake plot depicting the β scores across 593 E3-ligase-related gene identified in PC9 lung cancer cells treated with ABL kinase inhibitor under hypoxia. (*C*) IB analysis of IP- and WCL-derived HEK293T cells transfected with 3xFlag-HIF1A and HA-CPSF1 constructs for 24 h and then treated with MG132 during hypoxia for 24 h before harvesting. (*D*) IB analysis of WCL derived from HEK293T cells transfected with 3xFlag-HIF1A and HA-CPS1 constructs for 24 h and then exposed to normoxia or hypoxia for 24 h. (*E*) IB analysis of WCL derived from HEK293T cells transfected with 3xFlag-HIF1A and HA-CPSF1 constructs for 24 h and then treated with or without MG132 during hypoxia for 24 h before harvesting. (*F*) IB analysis of IP derived from HEK293T cells transfected with 3xFlag-HIF1A and HA-CSPF1 constructs for 24 h and then treated with MG132 for the final 24 h. (*G*) Proposed model depicting CPSF1-dependent HIF-1α ubiquitination and proteasome-mediated protein degradation.

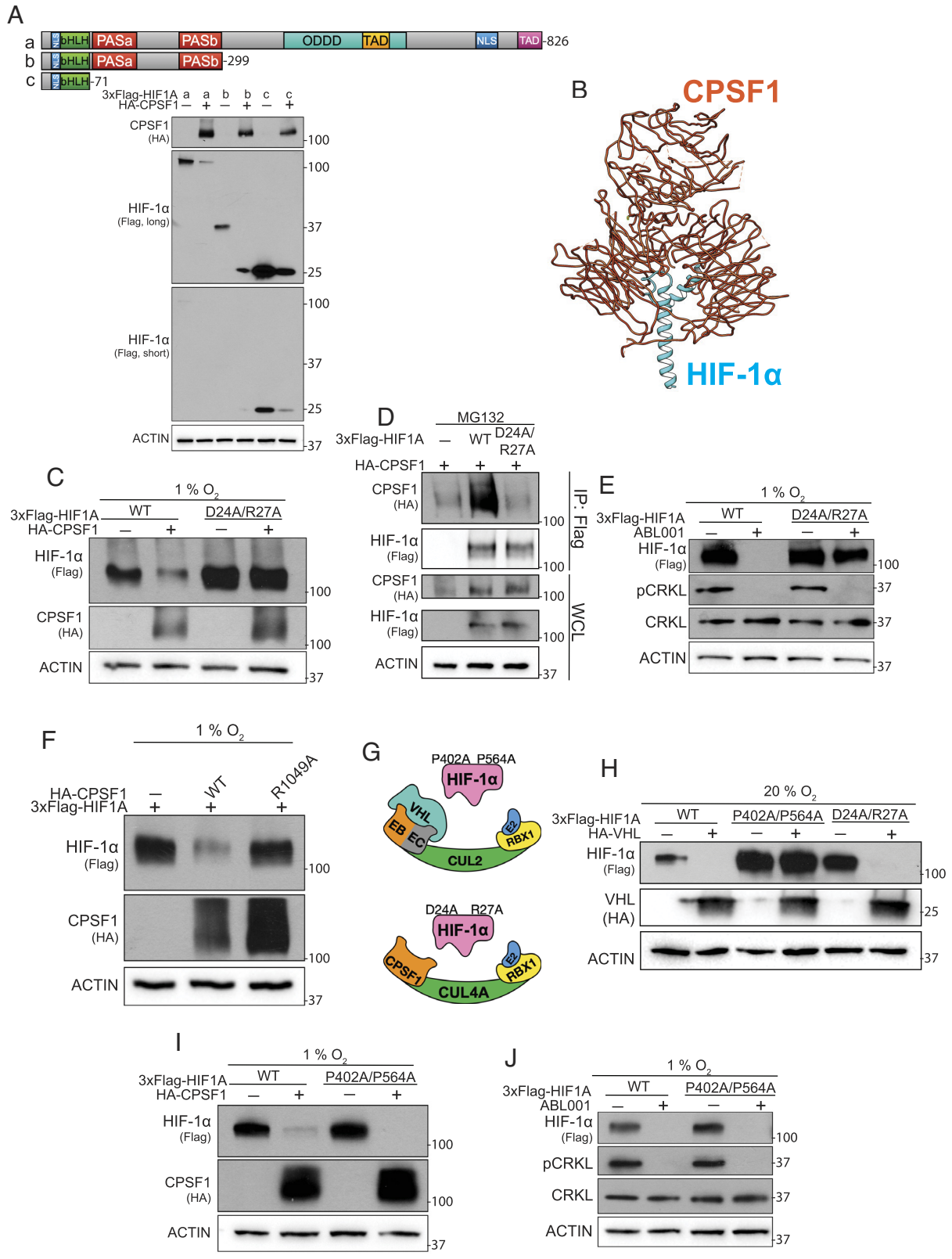

Fig. 5. CPSF1 is an E3-ligase targeting the HIF-1α DNA-binding domain. (*A*, *Top*) Structural diagram of full-length HIF-1α and truncation mutants. (*A*, *Bottom*) IB analysis of WCL derived from HEK293T cells transfected with HA-CPSF1 and indicated 3xFlag-HIF1A truncation constructs for 24 h and exposed to hypoxia for 24 h. (*B*) HDOCK protein–protein docking server prediction of the interaction of full-length CPSF1 (PDB: 6F9N) with HIF-1α AA 1-71 (PDB:4ZPR). CPSF1 is shown in orange and HIF-1α is shown in blue. (*C*) IB analysis of WCL derived from HEK293T cells transfected with indicated 3xFlag-HIF1A and HA-CPSF1 constructs for 24 h and exposed to hypoxia for 24 h. (*D*) IB and IP analysis of WCL derived from HEK293T cells transfected with HA-CPSF1 and indicated 3xFlag-HIF1A constructs for 24 h and exposed to hypoxia for 24 h. (*E*) IB analysis of WCL-derived 293T cells transfected with indicated 3xFlag-HIF1A constructs for 24 h and then treated with or without ABL001 during hypoxia for 24 h. (*F*) IB analysis of WCL derived from HEK293T cells transfected with 3xFlag-HIF1A and indicated HA-CPSF1 constructs for 24 h and exposed to hypoxia for 24 h. (*G*) Scheme of CPSF1- and VHL-resistant HIF-1α mutants. (*H*) IB analysis of WCL derived from HEK293T cells transfected with indicated 3xFlag-HIF1A and HA-VHL constructs for 24 h and exposed to hypoxia for 24 h. (*I*) IB analysis of WCL derived from HEK293T cells transfected with indicated 3xFlag-HIF1A and HA-CPSF1 constructs for 24 h and exposed to hypoxia for 24 h. (*J*) IB analysis of WCL-derived 293T cells transfected with indicated 3xFlag-HIF1A constructs for 24 h and then treated with or without ABL001 during hypoxia for 24 h.

residues (HIF-1α D24A/R27A) resulted in a HIF-1α protein that was not susceptible to degradation by CPSF1 (Fig. 5*C*, lanes 2 and 4). Further, HIF-1α D24A/R27A failed to coimmunoprecipitate with CPSF1 (Fig. 5*D*). Notably, the HIF-1α D24A/R27A mutant, which is no longer regulated by CPSF1, is also resistant to ABL kinase inhibitor-induced degradation (Fig. 5*E*). HIF-1α D24 is predicted to pair with CPSF1 R1049 using the HDOCK program (Fig. 5*B*). We tested this prediction and found that the CPSF1 R1049A mutant did not induce HIF-1α turnover (Fig. 5*F*).

Our data revealed that a HIF-1α D24A/R27A mutant is resistant to CPSF1-dependent degradation (Fig. 5 *C* and *G*). Others reported that a HIF-1α P402A/P564A is resistant to VHL-dependent degradation (3) (Fig. 5*G*). Consistent with this report, we found that expression of VHL led to profound loss of WT HIF-1α protein levels but failed to degrade the HIF-1α P402A/P564A mutant protein (Fig. 5*H*). In contrast, VHL expression down-regulated the HIF-1α D24A/R27A mutant protein that is resistant to CPSF1-induced degradation (Fig. 5*H*). These data support the model that VHL and CPSF1 regulate HIF-1α protein stability through distinct binding sites. Further support for this model is provided by our finding that CPSF1 expression was sufficient to decrease HIF-1α P402A/P564A protein levels (Fig. 5*I*). Further, while ABL kinase inhibition failed to down-regulate the HIF-1α D24A/R27A mutant, ABL inhibition decreased expression of the HIF-1α P402A/P564A mutant to the same extent as HIF-1α wild type (Fig. 5 *E* and *J*). Together, these results support a role for an ABL-dependent CPSF1 E3-ligase-targeting HIF-1α.

ABL Kinase Activity Protects HIF-1α from CPSF1-Dependent Degradation. To determine whether CPSF1 is the E3-ligase responsible for ABL inhibitor-dependent HIF-1α turnover, we generated pools of cells (in the PC9 and HEK293T cell background) in which CPSF1 was knocked out using CRISPR/Cas9. In these CPSF1-depleted cells, HIF-1α protein is stabilized and is rendered insensitive to ABL kinase inhibition. (Fig. 6*A*). Further, expression of ABL1 reversed the CPSF1-dependent loss of HIF-1α (Fig. 6*B*). Moreover, endogenous CPSF1 and HIF-1α only formed a detectable complex in cells after treatment with an ABL kinase inhibitor (Fig. 6*C*). These data are consistent with the model that active ABL kinases support the stabilization of HIF-1α by inhibiting CPSF1 E3-ligase activity (Fig. 6*D*).

ABL Interacts with and Phosphorylates CUL4A. Because ABL tyrosine kinase activity is necessary to protect HIF-1α from CPSF1-dependent degradation, we next investigated whether HIF-1α and/or CPSF1 might be tyrosine phosphorylated by ABL1. We did not detect ABL-dependent phosphorylation of either protein (*SI Appendix*, Fig. S9). Unexpectedly, mining the BioGRID database revealed that both ABL1 and ABL2 could interact with the cullin adaptor CUL4A, which might function as a potential CPSF1-scaffold protein in an E3 ligase complex (25, 28). Indeed, we found that endogenous ABL1 and ABL2 coimmunoprecipitated with endogenous CUL4A (Fig. 7 *A*–*C*). Importantly, the interaction between ABL kinases and CUL4A was impaired by treatment of lung cancer cells with ABL001 (Fig. 7 *A*–*C* and *SI Appendix* Fig. S10*A*).

To characterize the interaction between the ABL kinases and CUL4A, we coexpressed eGFP-tagged ABL1 WT, kinase-inactive (K290M), SH2-defective (R171K), and SH3-defective (P131L) proteins with Flag-tagged CUL4A. While WT and SH3-defective ABL1 proteins strongly coimmunoprecipitated with Flag-tagged CUL4A, the SH2-defective ABL1 protein interacted with CUL4A to a lesser extent (Fig. 7*D*). Notably, the kinase-inactive ABL1 K290M protein did not interact with CUL4A. These findings suggest that the interaction between the ABL kinases and CUL4A is dependent on ABL kinase activity. To identify the region of CUL4A required for its interaction with ABL1, we generated CUL4A truncation mutants (Fig. 7*E*). We found that the CUL4A DDB1 interaction site (IS) domain is necessary for interaction

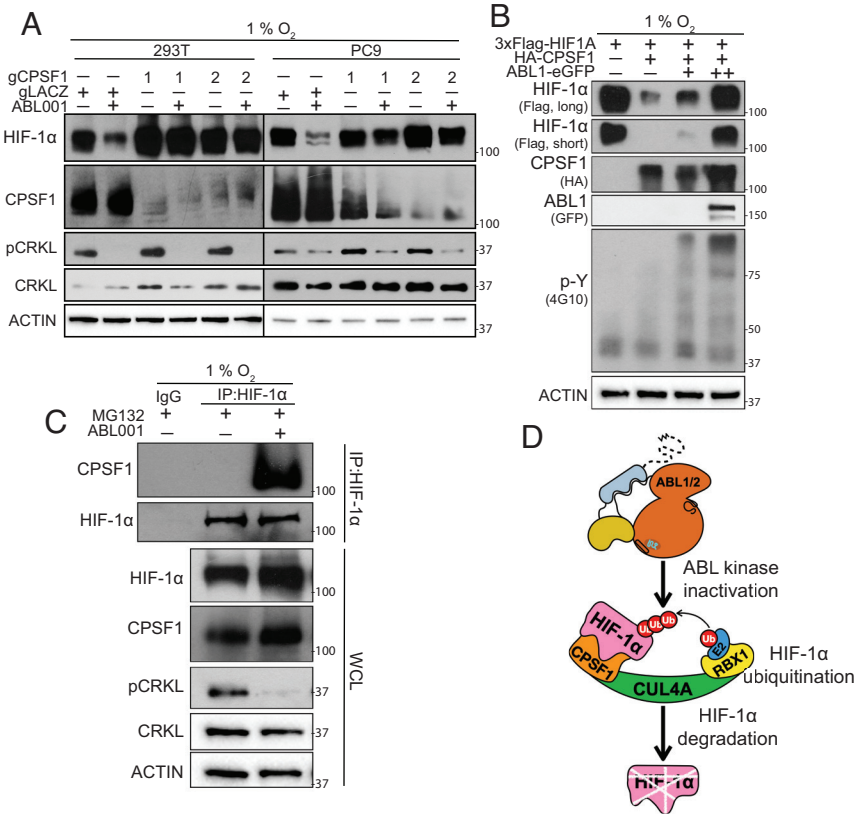

Fig. 6. ABL kinases protect HIF-1α from CPSF1-dependent degradation. (*A*) IB analysis of WCL derived from HEK293T and PC9 cells transduced with indicated gRNA/CRISPR-Cas9 constructs and then treated with ABL001 during hypoxia for 24 h. (*B*) IB analysis of WCL derived from HEK293T cells transfected with 3xFlag-HIF1A, ABL1-eGFP, and HA-CPSF1 constructs for 24 h and then exposed to hypoxia for 24 h. (*C*) IB and IP analysis of WCL derived from PC9 cells treated with ABL001 (24 h) and MG132 (final 6 h) during hypoxia for 24 h. IgG sample added to the vehicle and MG132-treated lysate. (*D*) Proposed model depicting loss of ABL kinase activity leading to CPSF1-dependent HIF-1α ubiquitination and proteasome-mediated protein degradation.

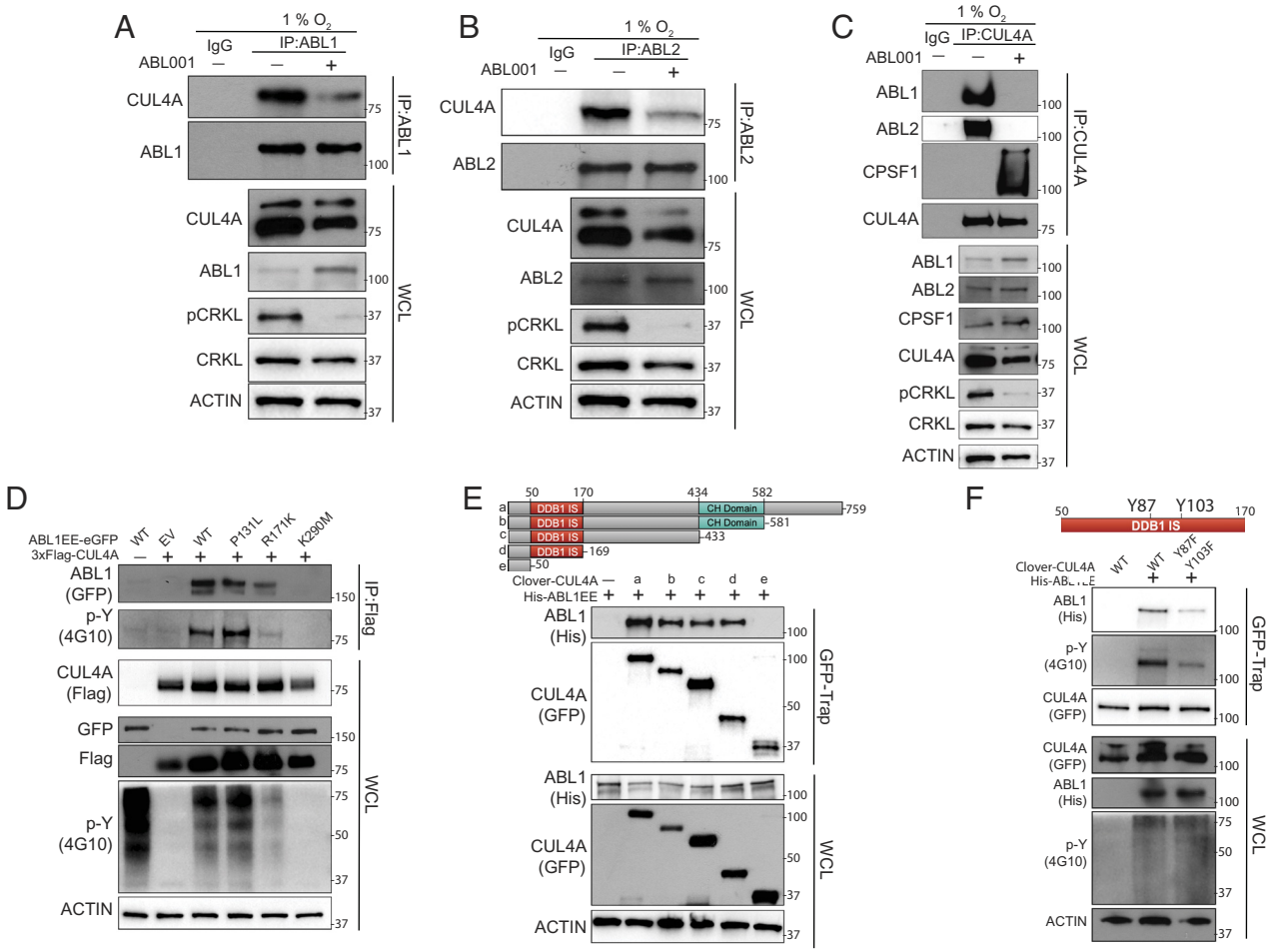

Fig. 7. ABL kinases interact with and phosphorylate CUL4A. (*A*–*C*) IB and IP analysis of WCL of indicated endogenous ABL and CUL4A proteins from PC9 cells treated with or without ABL001 (24 h) during hypoxia for 24 h. Cell lysates were incubated with IgG control or indicated antibodies. (*D*–*F*) IB analysis of IP- and WCL-derived HEK293T cells transfected with indicated epitope-tagged CUL4A and ABL1 constructs for 24 h and then exposed to hypoxia for 24 h before harvesting. DDB1 IS = DDB1 interaction site; CH domain = Cullin homology domain.

with His-tagged ABL1 as deletion of the CUL4A DDB1 IS domain impairs binding to ABL1 (Fig. 7*E*).

Because ABL kinase activity is necessary for interaction with CUL4A, we evaluated whether CUL4A is an ABL substrate. Indeed, coexpression active ABL1-EE resulted in a marked increase of CUL4A tyrosine phosphorylation (Fig. 7*D* and *SI Appendix* Fig. S9). As ABL1 interacts with the CUL4A DDB1 IS domain (Fig. 7*E*), we reasoned that the site(s) of ABL-mediated CUL4A tyrosine phosphorylation may localize within this domain. Therefore, we generated phosphorylation-deficient tyrosine to phenylalanine mutants for the five tyrosine residues (Y58, Y81, Y87, Y103, and Y160) located within the DDB1 IS domain (*SI Appendix* Fig. S10*B*). Both the CUL4A Y87F and Y103F mutants demonstrated a partial reduction in ABL1-dependent tyrosine phosphorylation (*SI Appendix* Fig. S10*B*). Importantly, the CUL4A Y87F/Y103F double mutant exhibited a marked decrease in binding to ABL1, as well as ABL1-dependent tyrosine phosphorylation (Fig. 7*F*). Together, these data demonstrate that the CUL4A scaffold protein is an ABL1 substrate and interacts with the ABL kinases in a kinase-domain and SH2-dependent manner.

ABL Kinase and CPSF1 Form Mutually Exclusive Complexes with CUL4A. To evaluate whether CUL4A might function as a scaffold protein to recruit CPSF1, we performed reciprocal coimmunoprecipitation of endogenous CPSF1 and CUL4A during Hx. Interestingly, we were only able to detect a complex between endogenous CPSF1 and CUL4A after ABL kinase inhibition (Figs. 6*C* and 8*A*). Interestingly, the CUL4A DDB1 IS domain, which mediates interaction with ABL1, is also necessary for interaction with CPSF1 (Fig. 8*B*). This finding suggested that ABL1 and CPSF1 may form mutually exclusive complexes with CUL4A. To assess this possibility, we examined whether expression of active ABL1 might disrupt CPSF1 binding to CUL4A. Indeed, while we readily detected an interaction between CUL4A and CPSF1, coexpression of active ABL1 resulted in disruption of the CUL4A-CPSF1 complex and formation of a CUL4A-ABL1 complex (Fig. 8*C*). Collectively, these data support the model that during Hx, active ABL kinases phosphorylate and interact with CUL4A and compete with CPSF1 for binding to the same CUL4A DDB1 IS site, thereby promoting increased HIF-1α protein expression (Fig. 8*D*). Conversely, upon ABL kinase inhibition, the ABL1–CUL4A interaction is disrupted leading to increased formation of the CPSF1-CUL4A E3-ligase complex, and subsequent HIF-1α ubiquitination and proteasomal-mediated degradation of HIF-1α (Fig. 8*D*).

ABL Kinases Protect MYC from CPSF1-Dependent Degradation. CPSF1 is likely to target additional E3-ligase substrates beyond HIF-1α. A proteomic dataset generated in U2OS cells revealed that MYC might be a potential CPSF1 interactor (25, 29). Notably, we previously demonstrated that ABL kinase inhibition or genetic depletion in lung cancer cells resulted in a decrease of MYC protein accumulation through an unknown mechanism

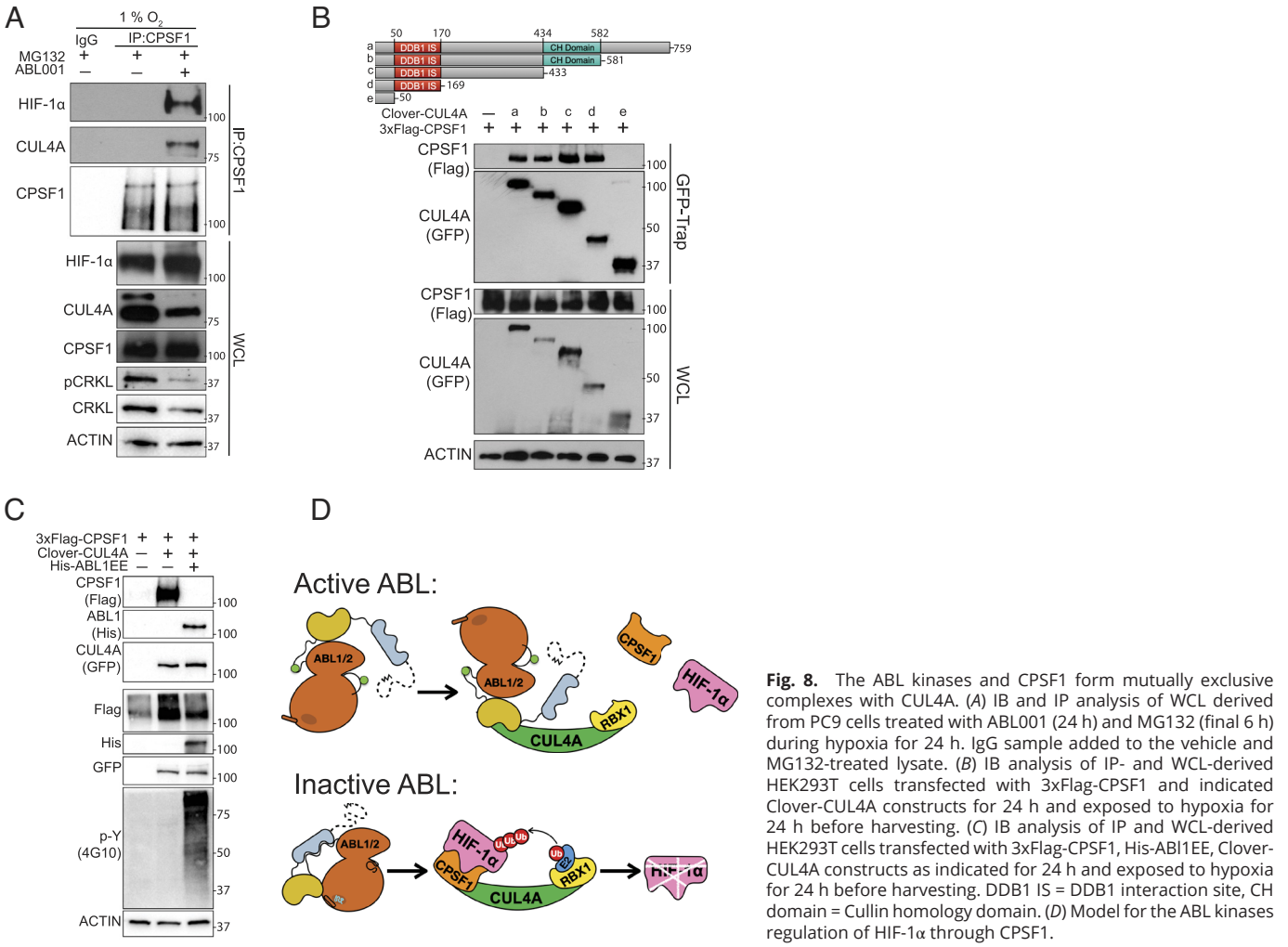

Fig. 8. The ABL kinases and CPSF1 form mutually exclusive complexes with CUL4A. (*A*) IB and IP analysis of WCL derived from PC9 cells treated with ABL001 (24 h) and MG132 (final 6 h) during hypoxia for 24 h. IgG sample added to the vehicle and MG132-treated lysate. (*B*) IB analysis of IP- and WCL-derived HEK293T cells transfected with 3xFlag-CPSF1 and indicated Clover-CUL4A constructs for 24 h and exposed to hypoxia for 24 h before harvesting. (*C*) IB analysis of IP and WCL-derived HEK293T cells transfected with 3xFlag-CPSF1, His-ABl1EE, Clover-CUL4A constructs as indicated for 24 h and exposed to hypoxia for 24 h before harvesting. DDB1 IS = DDB1 interaction site, CH domain = Cullin homology domain. (*D*) Model for the ABL kinases regulation of HIF-1α through CPSF1.

(14). We mapped the site of regulation on HIF-1α by CPSF1 to the HIF-1α bHLH DBD (Fig. 5). Interestingly, MYC, like HIF-1α, is a bHLH transcription factor that functions to induce expression of genes that drive cancer pathobiology (30). Indeed, we showed that CPSF1 coimmunoprecipitates with MYC in the presence of the MG132 proteasome inhibitor, and that increased expression of CPSF1 led to a dose-dependent loss of MYC protein levels that was reversed upon proteasomal inhibition (Fig. 9 *A*–*C*). Importantly, we found that the bHLH DBD of MYC is necessary for CPSF1 regulation of MYC protein accumulation as deletion of this domain ablated CPSF1-dependent degradation (Fig. 9*D*). Further, activation of ABL1 led to an increase in MYC protein levels (Fig. 9*E*). Moreover, treatment with ABL kinase inhibitors decreased endogenous and exogenous MYC protein levels in a proteasome-dependent manner under normoxic conditions (Fig. 9 *F*–*H*). Further, expression of exogenous-activated ABL1-EE reversed the CPSF1-dependent degradation of MYC (Fig. 9*I*). Together, these studies highlight a previously unknown ABL-CPSF1-dependent mechanism for regulating both MYC and HIF-1α protein levels (Fig. 9*J*).

Discussion

The mechanism governing the normoxic turnover of HIF-1α by oxygen-dependent prolyl-hydroxylation, ubiquitination by the VHL E3-ligase complex, and degradation by the 26S proteasome is well understood and validated (1–5). In contrast, much less is known about the processes that maintain HIF-1α protein levels during Hx beyond inactivation of PHD1-3 (8). Our studies revealed that ABL kinase activity is necessary for the maintenance of HIF-1α during Hx. The ABL nonreceptor tyrosine kinases are central signal transducers that are commonly exploited by cells to survive environmental and chemical stresses (12, 31). We report that ABL kinase activity becomes elevated in Hx and is necessary for the hypoxic accumulation of HIF-1α. Treatment with allosteric or orthosteric ABL kinase inhibitors leads to a striking loss of HIF-1α protein levels in multiple cell and cancer types during Hx. Moreover, knockdown of the ABL kinases individually or together ablates hypoxic HIF-1α protein levels. Conversely, activation of the ABL kinases by point mutations or treatment with an allosteric activator is sufficient to decrease HIF-1α ubiquitination and increase total HIF-1α levels. The ABL kinases and HIF-1α have both been implicated in the regulation of cellular processes such as lung injury and regeneration, as well as brain metastases which are linked to tissue Hx (9, 32–34). Our findings demonstrate that the ABL kinases are a druggable node that can be utilized to modulate HIF-1α protein levels in pathologies associated with Hx.

We employed an unbiased approach to identify the ABL-dependent E3-ligase(s) regulating HIF-1α protein stability. A FACS-based CRISPR/Cas9 screen using a custom E3-ligase targeted sgRNA library revealed CPSF1 as the ABL-dependent E3 ligase regulator targeting HIF-1α protein. CPSF1 is an understudied protein whose primary function is to serve as a core scaffolding component of the CPSF complex involved in 3′-polyadenylation of eukaryotic pre-mRNAs (21). Even though CPSF1 shares significant structural similarity with the known E3-ligase component DDB1 and CPSF1 complexes have been

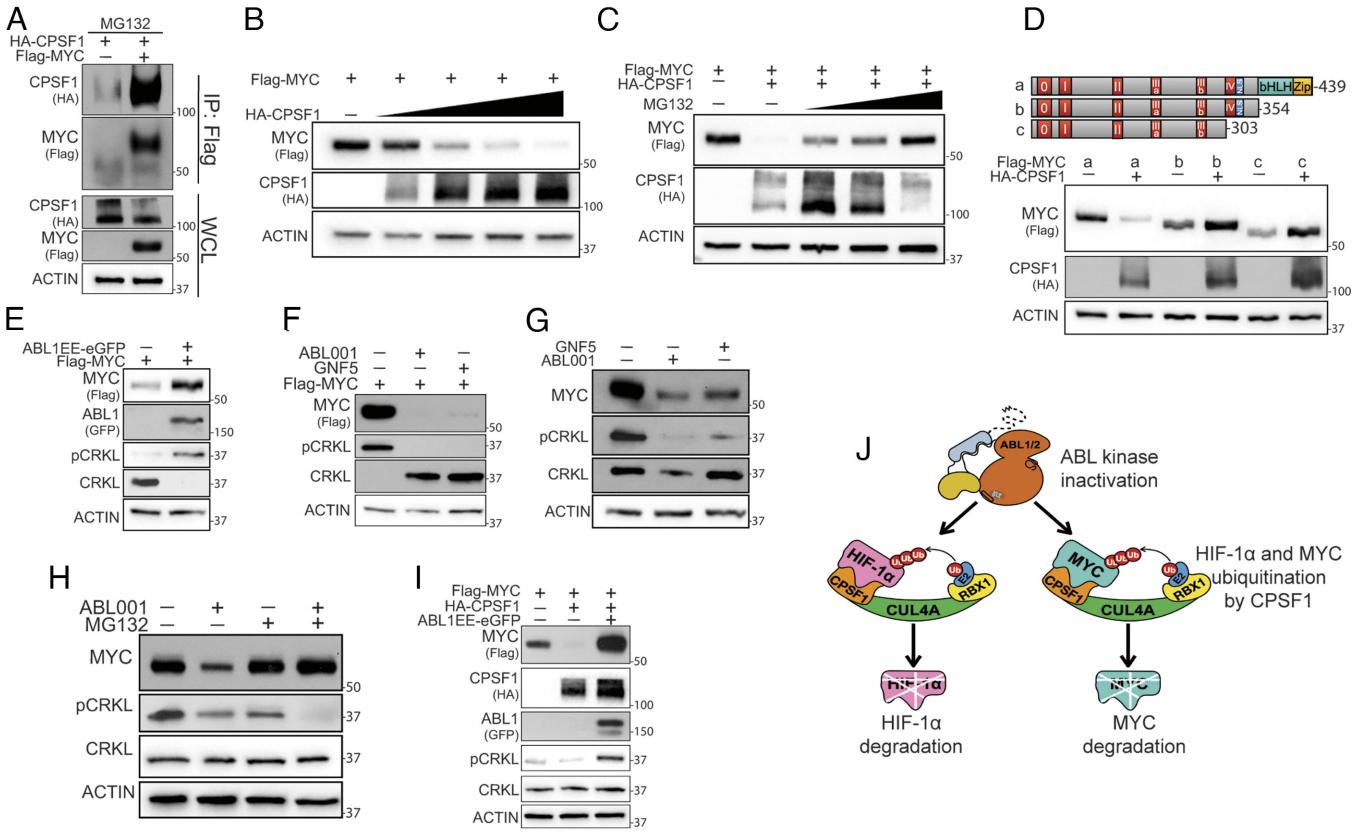

Fig. 9. ABL kinase protects MYC from CPSF1-dependent degradation. (*A*) IB analysis of IP- and WCL-derived HEK293T cells transfected with Flag-MYC and HA-CPSF1 constructs for 48 h. (*B*) IB analysis of WCL derived from HEK293T cells transfected with Flag-MYC and HA-CPSF1 constructs for 48 h. (*C*) IB analysis of WCL derived from HEK293T cells transfected with Flag-MYC and HA-CPSF1 constructs for 24 h and then treated with MG132 for 24 h before harvesting during normoxia. (*D*, *Top*) Structural diagram of full-length MYC and truncation mutants. (*A*, *Bottom*) IB analysis of WCL derived from HEK293T cells transfected with HA-CPSF1 and indicated Flag-MYC truncation constructs for 24 h and exposed to hypoxia for 24 h. (*E*) IB analysis of WCL derived from HEK293T cells transfected with Flag-MYC and ABL1-eGFP constructs for 48 h during normoxia. (*F*) IB analysis of WCL derived from HEK293T cells transfected with Flag-MYC for 24 h and then treated with ABL001 and GNF5 as indicated for 24 h during normoxia. (*G* and *H*) IB analysis of WCL derived from PC9 cells treated with ABL001, GNF5, and MG132 as indicated for 24 h during normoxia. (*I*) IB analysis of WCL derived from HEK293T cells transfected with Flag-MYC, ABL1-eGFP, and HA-CPSF1 constructs for 48 h. (*J*) Model for the ABL kinase regulation of HIF-1α and MYC through CPSF1.

shown to possess in vitro E3-ligase activity (23, 24), the identity of CPSF1 E3-ligase substrates was unknown.

In this study, we demonstrated that CPSF1 interacts with HIF-1α in cells in the presence of a proteasomal inhibitor. Ectopic expression of CPSF1 resulted in increased ubiquitination and proteasomal-dependent degradation of HIF-1α. We mapped the interaction site of CPSF1 on HIF-1α to the HIF-1α DBD. Using in silico docking of the HIF-1α DBD onto CPSF1 followed by in vitro validation, we identified that amino acids D24 and R27 on HIF-1α and R1049 on CPSF1 are essential for the interaction. The site of interaction on HIF-1α (D24 and R27) is flanked by two mutation cluster regions found in patients' tumors reported in the TCGA database (35). Even though genetic mutations in other genes have been shown to alter HIF-1α levels, few studies have investigated the impact of mutations in the *HIF1A* gene. Future studies evaluating the impact of these mutations on the CPSF1-dependent regulation of HIF-1α may be relevant in hypoxic disease settings. Further, we demonstrate that ABL kinases antagonize CPSF1-dependent degradation of HIF-1α as overexpression of active ABL1 reversed the loss of HIF-1α after CPSF1 expression.

Tyrosine phosphorylation has been shown to regulate the proteasomal degradation of substrates through multiple mechanisms including 1) phosphorylation of the substrate itself, 2) phosphorylation of the E3-ligase substrate receptor, and 3) phosphorylation of E3-ligase scaffolding proteins (36–38). Protein tyrosine kinases can promote the activation of signaling cascades that target multiple steps of the ubiquitin-proteasomal degradation pathway (37–39). The ABL kinases and ABL-fusion proteins can regulate the stability of target proteins through direct tyrosine phosphorylation of substrates or activation of serine/threonine protein kinase signaling cascades (12, 17, 31, 40). Here, we uncovered that ABL-meditated inactivation of the CPSF1-E3-ligase complex is mediated by phosphorylation of the CPSF1-scaffold protein CUL4A. We showed that CUL4A interacts with the ABL kinases in Hx, and that this interaction is lost upon ABL kinase inhibition. Using ABL domain-impaired mutants, we demonstrated that ABL kinase and phospho-tyrosine binding activities are necessary for interaction with CUL4A. Further, we determined that the major sites of ABL kinase phosphorylation on CUL4A are two tyrosine residues (Y87 and Y103) located within the DDB1 IS domain of CUL4A.

The interaction between endogenous CPSF1 and CUL4A was only detected after ABL kinase inhibition. We demonstrated that the DDB1 IS domain of CUL4A is essential for interaction with both CPSF1 and ABL. Since the ABL kinases and CPSF1 interact with the same domain on CUL4A and the endogenous complexes are detected under distinct ABL kinase activity states, we hypothesized that CPSF1 and ABL kinases form mutually exclusive complexes with CUL4A. Indeed, coexpression of active ABL1 was sufficient to disrupt the interaction of CUL4A with CPSF1. Thus, our data support a model in which active ABL kinases phosphorylate and interact with CUL4A, thereby preventing the formation of a CPSF1-CUL4A E3-ligase complex (Fig. 8*D*). Further, upon ABL kinase inhibition, formation of the ABL-CUL4A complex is impaired, allowing for

increased formation of the CPSF1-CUL4A complex, leading to polyubiquitination of HIF-1α and its proteasomal degradation.

Notably, we identified the MYC oncoprotein as a second CPSF1- E3 ligase substrate. The BioGRID database was employed to find potential CPSF1 interactors, which revealed an uncharacterized interaction between CPSF1 and MYC (25, 29). MYC, like HIF-1α, belongs to the family of bHLH transcription factors and is commonly coopted by cancer cells to drive expression of genes essential for tumor development and progression (30). We demonstrated that CPSF1 interacts with MYC. Further, expression of CPSF1 or loss of ABL kinase activity resulted in the proteasome-mediated degradation of MYC. Conversely, activation of ABL1 was able to reverse the CPSF1-dependent loss of MYC. Importantly, similar to the HIF-1α bHLH, we found that the MYC bHLH domain is the site of CPSF1-mediated regulation.

We identified two substrates of the CPSF1 E3-ligase complex using a hypothesis-driven approach. Future work is needed to interrogate the CPSF1-mediated degradome using unbiased proteomics approaches to identify additional CPSF1 substrates. The two substrates we identified, HIF-1α and MYC, are bHLH transcription factors (41), and the site of regulation by CPSF1 is the bHLH DBD in both HIF-1α and MYC. The bHLH transcription factor in humans contains over 130 family members divided into five families (A, B, C, D, and E). HIF-1α and MYC are found on different branches of the same E family (41). It would be of interest to determine whether additional bHLH transcription factors are CPSF1 substrates, and, if so, whether these substrates cluster in the E family or other distinct families. As we identified that the CPSF1-dependent regulation of HIF-1α and MYC is antagonized by ABL kinase activity, it will be of interest to investigate whether the stability of additional bHLH factors is also ABL dependent. ABL1 is a component of the constitutively active fusion oncoprotein BCR-ABL1, which is the oncogenic driver of chronic myeloid leukemia (CML) (12). The loss of BCR-ABL1 kinase activity has previously been shown to decrease both MYC and HIF-1α protein levels in CML cell lines (42, 43). We therefore questioned whether BCR-ABL1 antagonized the CPSF1-dependent degradation of MYC and HIF-1α. However, unlike the adherent cell lines PC9 and HEK293T which can survive CPSF1 gRNA expression, the CML BCR-ABL1-positive cell lines K-562 and MEG-01 did not survive loss of CPSF1 expression upon transduction with lentiviruses encoding CPSF1-specific gRNAs or shRNAs. Notably, oncogenic activation of ABL kinases in the absence of chromosomal translocations is observed in solid tumors with high-level expression and activation of ABL kinases downstream of oncogenic tyrosine kinases, Hx, or metabolic stress (12). Our findings suggest that dynamic regulation of the CPSF1-CUL4A complex by ABL kinases might contribute to the regulation of MYC and HIF-1α protein stability and their oncogenic activities in selected solid tumors.

Materials and Methods

Cell Lines and Cell Culture Methods. HEK293T, MDA-MB-231, and SUM159 cells were purchased from American Type Culture Collection (ATCC). PC9 and H2030 cells were gifts from Joan Massagué (Memorial Sloan Kettering Cancer Center, New York). H460 cells were gifts from Fernando Lecanda (University of Navarra, Pamplona, Spain). The HEK293T cells and MDA-MB-231 cells were maintained in Dulbecco's Modified Eagle's Medium (DMEM) (Life Technologies) supplemented with 10% fetal bovine serum (FBS). The SUM159 cells were maintained in Ham's F-12 Nutrient Mix (ThermoFisher) supplemented with 10% FBS, 10 mM Hepes, 5 μg/mL insulin, and 1 μg/mL hydrocortisone. The PC9 and H2030 cells were maintained in RPMI 1640 (Life Technologies) supplemented with 10% FBS, 10 mM Hepes, 1 mM sodium pyruvate, and 0.2% glucose. All cells were grown at 37 °C in 5% CO_2 with either 1% or 20% O_2. Transient transfections were performed using Lipofectamine 2000 (Invitrogen) according to the manufacturer's instructions. Media was changed 24 h post transfection and cells were harvested 24 h thereafter. Generation of lentivirus and transductions of target cell lines were performed as described previously (4, 10). Transduced cells were selected with 1 μg/mL puromycin.

For experiments assessing effects of pharmacologic agents in vitro, drugs were dissolved in dimethyl sulfoxide (DMSO) unless indicated elsewise, with the final concentration of DMSO in culture media not exceeding 0.1% vol/vol. ABL001, GNF5, and Nilotinib were synthesized by the Duke University Small Molecule Synthesis Facility and were validated by 1H-NMR techniques and liquid chromatography–mass spectrometry. DPH [5-(1,3-diaryl-1H-pyrazol-4-yl) hydantoin, 5-[3-(4-fluorophenyl)-1-phenyl-1H-pyrazol-4-yl]-2,4-imidazolidinedione] (Sigma) was dissolved in DMSO. The proteasomal inhibitor MG132 (Selleckchem) was dissolved in DMSO. The Hx mimetic cobalt chloride ($CoCl_2$) (Sigma) was dissolved in water. All drugs were treated at concentrations indicated in figures and figure legends.

Plasmid Construction. The following plasmids were obtained from Addgene: HA-HIF1alpha-pcDNA3 (#18949), pCMV4a-Flag-c-Myc (#102625), pcDNA3-myc3-CUL4A (#19951), pcDNA3-myc3-CUL4B (#19922), pCI-His-hUbi (#31815), 3xFLAG-FUS-WT (#44985), HA-VHL-pRc/CMV (#19999), HA-Clover (#163366), pcDNA3.1-HA (#128034). The pCMV-CPSF1-Flag-Myc (C203519) plasmid was purchased from Origene. The shRNA constructs targeting the ABL kinases were described previously (4). The pN1-ABL1 and ABL2 constructs were described previously (4).

All constructs were confirmed by Sanger sequencing. The 3xFlag-HIF1A, CPSF1, and CUL4A constructs were generated by PCR amplification of HIF1A cDNA from HA-HIF1alpha-pcDNA3, CPSF1 cDNA from pCMV-CPSF1-Flag-Myc, and CUL4A from the pcDNA3-myc3-CUL4A plasmids prior to subcloning into the 3xFLAG-FUS-WT vector via restriction enzyme digestion. The HA-CPSF1 construct was generated by PCR amplification of CPSF1 cDNA from the pCMV-CPSF1-Flag-Myc plasmid and subcloned into the pcDNA3.1-HA construct after restriction enzyme digestion. The HA-Clover-CUL4A construct was generated by PCR amplification of CUL4A cDNA from the pcDNA3-myc3-CUL4A plasmid and subcloned into the HA-Clover construct after restriction enzyme digestion.

The CPSF1 targeting gRNA-CRISPR/Cas9 lentiCRISPR2 constructs were generated using the Zhang lab protocol. The sgRNA sequences are listed below (5′-3′):

sgCPSF1 #1
1) FWD: AAGAAGCGAGTGGATGCGAG
2) REV: CTCGCATCCACTCGCTTCTT

sgCPSF1 #2
3) FWD: TACAGCGTGGACTTCATGGG
4) REV: CCCATGAAGTCCACGCTGTA

The following constructs were generated by using the QuickChange Lightning site-directed mutagenesis kit (Stratagene) according to the manufacturer's protocol. Mutagenesis primers are listed below (5′-3′):

HIF-1 α Constructs. D24A and R27A on the 3xFlag-HIF1A plasmid
5) FWD: TCTTTACTTCGCCGAGATGCGGCTGCAGCTCGAGACTTTTCTTTTC
6) REV: GAAAAGAAAAGTCTCGAGCTGCAGCCGCATCTCGGCGAAGTAAAGA

P402A on the 3xFlag-HIF1A plasmid
1) FWD: CTCCAGCGGCTGCGGCCAGCAAAGT
2) REV: ACTTTGCTGGCCGCAGCCGCTGGAG

P564A on the 3xFlag-HIF1A P402A plasmid
1) FWD: CCATTGGGATATAGGCAGCTAACATCTCCAAGTCTAA
2) REV: TTAGACTTGGAGATGTTAGCTGCCTATATCCCAATGG

L72(STOP) on the 3xFlag-HIF1A plasmid
1) FWD: ATCACCAGCATCCAGCTATTTCCTCACACGCAAATAGCTGATGGT
2) REV: ACCATCAGCTATTTGCGTGTGAGGAAATAGCTGGATGCTGGTGAT

Q299(STOP) on the 3xFlag-HIF1A plasmid
1) FWD: GTACTGTCCTGTGGTGACTTATCCTTTAGTAAACATATCATG
2) REV: CATGATATGTTTACTAAAGGATAAGTCACCACAGGACAGTAC

ABL1 Constructs. P249E on the pN1-ABL1 WT-eGFP plasmid (PE mutant)
3) FWD: TCTCCCACTTGTCGTAGTTCTCGGACACACCATAGACAGTG
4) REV: GCCCCAAAGCGCAACAAGGAGACTGTCTATGGTGTGTCC

P242E on the pN1-ABL1 P249E-eGFP plasmid (PPEE mutant)
1) FWD: GGACACACCATAGACAGTCTCCTTGTTGCGCTTTGGGGC
2) REV: GCCCCAAAGCGCAACAAGGAGACTGTCTATGGTGTGTCC

P131L on the pN1-ABL1 P242/249E-eGFP plasmid
1) FWD: GGTGATGTAGTTGCTTAGGACCCATCCTTGGCC
2) REV: GGCCAAGGATGGGTCCTAAGCAACTACATCACC

R171K on the pN1-ABL1 P242/249E-eGFP plasmid
1) FWD: CAGGACTGCTCTCACTCTCCTTCACCAAGAAGCTGCCATTG

2) REV: CAATGGCAGCTTCTTGGTGAAGGAGAGTGAGAGCAGTCCTG

K290M on the pN1-ABL1 P242/249E-eGFP plasmid

1) FWD: CCTCCTTCAAGGTCATCACGGCCACCGTC

2) REV: GACGGTGGCCGTGATGACCTTGAAGGAGG

ABL2 Constructs. P276E on the pN1-ABL2 WT-eGFP plasmid (PE mutant)

3) FWD: CATTTCCCACTTGTCATGGATCTCAGACACGCCATAGACGGTTGG

4) REV: CCAACCGTCTATGGCGTGTCTGAGATCCATGACAAGTGGGAAATG

P269E on the pN1-ABL2 P276E-eGFP plasmid (PPEE mutant)

5) FWD: AGACACGCCATAGACGGTCTCCTTGTTGCACTTCGGTGC

6) REV: GCACCGAAGTGCAACAAGGAGACCGTCTATGGCGTGTCT

CPSF1 Constructs. R1049E on the HA-CPSF1 plasmid

1) FWD: CTCGCCAGTCATGGCTGGGATGCGGGCA

2) REV: TGCCCGCATCCCAGCCATGACTGGCGAG

CUL4A Constructs. Y58F on the Clover-CUL4A plasmid

1) FWD: CTGCCCGACAACTTCACGCAGGACACG

2) REV: CTGCCCGACAACTTCACGCAGGACACG

Y81F on the Clover-CUL4A plasmid

1) FWD: GCTCCTCGAGGTTGAACCTGATGGAGGTG

2) REV: CACCTCCATCAGGTTCAACCTCGAGGAGC

Y87F on the Clover-CUL4A plasmid

1) FWD: CACAGCCTGGAAGAGCTCCTCGAGGTTGTA

2) REV: TACAACCTCGAGGAGCTCTTCCAGGCTGTG

Y103F on the Clover-CUL4A plasmid

1) FWD: CTGACGCAGTTGCTTGAAGAGCATTGGGGAGAC

2) REV: GTCTCCCCAATGCTCTTCAAGCAACTGCGTCAG

Y160F on the Clover-CUL4A plasmid

1) FWD: GAGTTCTGCAGCACAAAGGTGCGGTCCAAGAAC

2) REV: GTTCTTGGACCGCACCTTTGTGCTGCAGAACTC

F582(STOP) on the Clover-CUL4A plasmid

1) FWD: GGAATTCCTTCTTCCCTTCTTTCTACTCCGCTTTTAAAACAGCATG

2) REV: CATGCTGTTTTAAAAGCGGAGTAGAAAGAAGGGAAGAAGGAATTCC

D434(STOP) on the Clover-CUL4A plasmid

1) FWD: GAACAGGATCATGATCTTCTACAACGTCCGCTCCAGCT

2) REV: AGCTGGAGCGGACGTTGTAGAAGATCATGATCCTGTTC

I170(STOP) on the Clover-CUL4A plasmid

1) FWD: GTTCTAATCCCATATCCCACTAGGAGGGCAGCGTGGAGTTC

2) REV: GAACTCCACGCTGCCCTCCTAGTGGGATATGGGATTAGAAC

R51(STOP) on the Clover-CUL4A plasmid

1) FWD: GGCAGCCGAGGTCAGTCTCGGAAGTTC

2) REV: GAACTTCCGAGACTGACCTCGGCTGCC

MYC Constructs. K355(STOP) on the Clover-CUL4A plasmid

1) FWD: TTGTGTGTTCGCCTCTAGACATTCTCCTCGGTG

2) REV: CACCGAGGAGAATGTCTAGAGGCGAACACACAA

T304(STOP) on the Clover-CUL4A plasmid

1) FWD: CTGCGTAGTTGTGCTGATGCTAGGAGACGTGGCACCTCTTG

2) REV: CAAGAGGTGCCACGTCTCCTAGCATCAGCACAACTACGCAG

Immunoblot (IB) and Immunoprecipitation Analyses. For IB analysis of whole-cell lysates (WCL), cells were lysed in RIPA lysis buffer [RIPA buffer (50 mM Tris-HCl pH 7.4, 150 mM NaCl, 1 mM EDTA, 1% Triton X-100, 1% sodium deoxycholate, and 0.1% sodium dodecyl sulfate (SDS) containing protease-phosphatase inhibitor cocktail (Cell Signaling). Lysates were rotated for 10 min at 4 °C and cell debris was cleared by centrifugation at 15,000 RPM for 10 min at 4 °C. Protein concentration was determined using the DC Protein Assay (Bio-Rad). For WCL, 25 μg of total proteins was loaded per well.

For ectopic immunoprecipitation analysis, cells were lysed in RIPA lysis buffer [RIPA buffer (50 mM Tris-HCl pH 7.4, 150 mM NaCl, 1 mM EDTA, 1% Triton X-100, 1% sodium deoxycholate, and 0.1% SDS containing protease-phosphatase inhibitor cocktail (Cell Signaling). Lysates were incubated on ice for 30 min and vortexed every ten minutes (30 min, 20 min, 10 min, and 0 min). Cell debris was cleared by centrifugation at 15,000 RPM for 10 min at 4 °C and protein concentration was determined using the DC Protein Assay (Bio-Rad). 1 mg of total protein was diluted to 800 μL and 200 μg of total protein was saved for later WCL immunoblotting. A volume of 20 μL anti-FLAG M2 or GFP-Trap affinity gel was added to each sample and rotated overnight (~16 h) at 4 °C. Beads were washed three times with RIPA lysis buffer. Immunoprecipitated proteins were eluted by boiling in 150 μL of 4× SDS Laemmli Sample Buffer (BioRad). For endogenous immunoprecipitation analysis, the protocol was performed as described previously (9, 13).

The immunocomplexes and WCL samples were separated by SDS-polyacrylamide gel electrophoresis (PAGE) and transferred onto nitrocellulose membranes using the Transblot Turbo Transfer system (Bio-Rad). The nitrocellulose membranes were blocked in 5 % milk in tris-buffered saline- Tween 20 (TBST) (20 mM Tris pH 7.6, 150 mM NaCl, and 0.1% w/v Tween 20 detergent) for 30 min at room temperature and then incubated in primary antibodies overnight. All antibodies were diluted in 5 % milk in TBST, except for HIF-1α, HIF-2α, HIF-1β, pCRKL, and 4G10, which were diluted in 5% BSA in TBST. The nitrocellulose membranes were washed 3 times with TBST and incubated in secondary antibodies diluted in 5% milk in TBST for 1 h. After washing 3 times in TBST, the blots were developed using either film or a ChemiDoc XRS+ imager (Bio-Rad).

The following primary antibodies were used for IB analyses: ABL1 (Sigma MAB1130 1:1,000), ABL2 (Abnova, H00000027-M03, 1:500), ACTIN (Cell Signaling 3700 1:10,000), CPSF1 (Bethyl A301-580A 1:1,000), CRKL (Santa Cruz sc-319 1:1,000), CRKL p-Y207 (Cell Signaling 3181 1:500), Flag (Sigma M2 1:5,000), GFP (Cell Signaling 2956 1:1,000), HA (Cell Signaling 2367 1:1,000), HIF-1α (BD Bioscience 610959 1:1,000), HIF-2α (Novus NB100-122 1:1,000), HIF-1β (Novus NB100-124 1:1,000), MYC (Cell Signaling 5605 1:5,000), Ubb (Santa Cruz sc-166553 1:1,000), and p-Y 4G10 (Sigma 05-321). The following secondary antibodies were used for IB analyses: Peroxidase AffiniPure Goat Anti-Mouse IgG (H+L) (Jackson Immunoresearch 115-035-003 1:2,000), AffiniPure Goat Anti-Mouse IgG (H+L) (Jackson Immunoresearch 115-035-1441:2,000), and TidyBlot (BioRad STAR209 1:500).

Real-Time Quantitative PCR. RNA was extracted and purified from cells using the RNeasy RNA Isolation Kit (QIAGEN). cDNA synthesis was generated by performing reverse transcription on 1 μg total RNA using oligo(dT) primers and M-MLV reverse transcriptase (Invitrogen). Quantitative PCR was performed using Taq Universal SYBR Green Supermix (Bio-Rad). Analysis was performed using the $2^{-\Delta\Delta Ct}$ method.

Luciferase Assay. Luciferase assay was performed using the Pierce Firefly Luciferase Glow Assay (Promega) according to the manufacturer-provided protocol. Cells were seeded into 96-well plates in triplicate and plates were read using a Tecan Infinite M1000 Microplate-Reader.

Proteasome Activity Assay. Proteasome activity assay was performed using the Proteasome activity Assay Kit (Sigma) according to the manufacturer-provided protocol. Cells were seeded into 96-well plates in triplicate and plates were read using a Tecan Infinite M1000 Microplate-Reader.

FACS Screen. A custom CRISPR sgRNA library targeting 593 known or predicted human E3 ligases (5 sgRNAs per gene, 2,965 total) and nontargeting controls (50 total) was designed and subsequently synthesized by Custom Array. The oligo pool was prepared and cloned into the lentiCRISPRv2 backbone (Addgene #52961) using Gibson assembly as described by Shalem et al., with minor modifications (31, 44, 45). Lentivirus was produced by transfecting HEK293FT cells with the lentiCRISPRv2 sgRNA library plasmid pool and psPAX2 (Addgene #12260) and pMD2.G (Addgene #12259) packaging plasmids using Lipofectamine 2000 and PLUS Reagent (Thermo) as previously described (44). After 6 h, the transfection mixture was replaced by harvest media (DMEM, 30% FBS). After 48 h, the virus-containing media was harvested, passed through a 0.45-μm low-binding filter, and aliquoted and stored at −80 °C. PC9 cells were seeded into nontissue culture-treated 6-well plates at a density of 2×10^6 cells/well with 8 μg/mL polybrene and transduced at a low multiplicity of infection ~0.3 via spinfection to achieve greater than 3,000× coverage of the sgRNA library. Immediately following spinfection, the cells were transferred from 6-well plates to 15 cm tissue culture dishes at a seeding density of 4×10^6 cells per plate and were allowed to recover. After 24 h, media was replaced with fresh media containing 2 μg/mL puromycin and cells selected for 48 h. The cells were passaged and maintained above 3,000× coverage for 7 d postspinfection to allow for stable integration and Cas9-directed knockout of target genes. The cells were then split into triplicate conditions (7.5×10^6 cells per replicate) and treated with 5 μM Nilotinib immediately prior to incubation in 1% O_2 for 24 h. After hypoxic incubation, the cells were fixed and permeabilized using the eBioscience Foxp3 Transcription Factor Staining Buffer Set (Thermo) according to manufacturer's recommendations, with minor modifications. Fixed and permeabilized cells were incubated overnight at 4 °C, rotating with a PE-conjugated HIF-1α antibody (BioLegend) at 5 μL per 1,000,000 cells. For each replicate, stained cells were then sorted by FACS, collecting the top and bottom 10% of HIF-1α-expressing cells on the basis of PE signal; the cells were collected in FBS-coated tubes, maintaining approximately 300× coverage per high and low population. An ungated control sample was also collected for each replicate.

Immediately thereafter, the collected samples were individually subjected to reverse-cross-linking and genomic DNA extraction using the Arcturus PicoPure DNA Extraction Kit (Thermo), according to manufacturer's recommendations. sgRNA libraries were PCR amplified from gDNA using NEBNext Ultra II Q5 Master Mix (New England BioLabs) according to manufacturer's instructions, using the following primers:

FWD 5′- AATGATACGGCGACCACCGAGATCTACACAATTTCTTGGGTAGTTTGCAGTT
ReV 5′- CAAGCAGAAGACGGCATACGAGAT (6 bp index sequence)
GACTCGGTGCCACTTTTTCAA

Amplified libraries were purified using SPRIselect beads (Beckman Coulter) using right-sided selection of 0.75× then to 1.2× the original volume. Each sample was quantified using the Quant-iT dsDNA Broad Range Assay Kit (Thermo). Samples were pooled and sequenced on a NextSeq 500 (Illumina) with 20 bp single-end sequencing using the following custom read and index primers:

Custom Read 5′- GATTTCTTGGCTTTATATATCTTGTGGAAAGGACGAAACACCG
Custom Index 5′- GCTAGTCCGTTATCAACTTGAAAAAGTGGCACCGAGTC

Raw sequencing read counts were trimmed and processed, and analysis of enrichment and depletion metrics comparing the top and bottom 10% sorted populations was performed using the MAGeCK software analysis pipeline under default settings.

Molecular Docking. The HIF-1α DBD (AA 1-71) (PDB:4ZPR) was docked onto full-length CPSF1 (PDB: 6F9N) using the HDOCK protein–protein docking server (http://hdock.phys.hust.edu.cn/). The predicted complexes with the highest scores were visualized using Chimera (University of California, San Francisco).

Statistics. Statistical differences between groups were determined using a repeated-measure ANOVA followed by post hoc testing (Tukey's). All statistical tests were performed in JMP and a *P* value of 0.05 was selected as the significance cutoff. All data shown indicated averages with SEM.

Data, Materials, and Software Availability. All data are available in the main text or the supporting information. CRISPR dataset has been deposited at Gene Expression Omnibus (GEO) and is publicly available as of the date of publication (BioProject ID: PRJNA945492) (46).

ACKNOWLEDGMENTS. We thank Dr. Joan Massagué (Memorial Sloan Kettering Cancer Center, New York, NY) for providing the PC9 and H2030 lung cancer cells. We thank the Duke Flow Cytometry Shared Resource for assistance with cell sorting, and the Duke Light Microscopy Core Facility. We thank Dr. Lynn Martinek, Dr. Wendi Guo, and Kassandra Spiller (Duke University, Durham, NC) for technical assistance. We thank Shane Killarney, Jude Raj, and members of the Pendergast laboratory at Duke University for helpful discussions. Funding: This study was financially supported by NIH grant R01CA246133 (A.M.P.), NIH grant 5R01HL151782 (A.M.P.), NIH grant P30CA014236 (A.M.P.), NIH grant R01CA266389 (K.C.W.), NIH grant R01CA263593 (K.C.W.), NIH grant F31CA243293 (B.M.), NIH grant F99CA264162 (B.M.), NIH grant 5T32GM007105 (B.M.), NIH grant K00CA245732 (J.P.H.), NIH grant F30CA247323 (C.G.C.-S.), Department of Defense grant W81XWH-22-10033 (A.M.P.), Department of Defense grant W81XWH-21-10362 (K.C.W.), Department of Defense grant W81XWH-19-10414 (K.C.W.), Department of Defense grant W81XWH-18-1-0064 (D.P.M.).

Author affiliations: [a]Department of Pharmacology and Cancer Biology, Duke University School of Medicine, Durham, NC 27710; [b]Duke Cancer Institute, Duke University School of Medicine, Durham, NC 27710; and [c]Department of Orthopedic Surgery, Duke University School of Medicine, Durham, NC 27710

1. W. G. Kaelin Jr., P. J. Ratcliffe, Oxygen sensing by metazoans: The central role of the HIF hydroxylase pathway. *Mol. Cell* **30**, 393–402 (2008).
2. W. G. Kaelin Jr., The von Hippel-Lindau tumour suppressor protein: O2 sensing and cancer. *Nat. Rev. Cancer* **8**, 865–873 (2008).
3. M. Ivan *et al.*, HIFalpha targeted for VHL-mediated destruction by proline hydroxylation: Implications for O2 sensing. *Science* **292**, 464–468 (2001).
4. P. Jaakkola *et al.*, Targeting of HIF-alpha to the von Hippel-Lindau ubiquitylation complex by O2-regulated prolyl hydroxylation. *Science* **292**, 468–472 (2001).
5. N. Masson, C. Willam, P. H. Maxwell, C. W. Pugh, P. J. Ratcliffe, Independent function of two destruction domains in hypoxia-inducible factor-alpha chains activated by prolyl hydroxylation. *EMBO J.* **20**, 5197–5206 (2001).
6. J. Lopez-Barneo, M. C. Simon, Cellular adaptation to oxygen deficiency beyond the Nobel award. *Nat. Commun.* **11**, 607 (2020).
7. P. Lee, N. S. Chandel, M. C. Simon, Cellular adaptation to hypoxia through hypoxia inducible factors and beyond. *Nat. Rev. Mol. Cell Biol.* **21**, 268–283 (2020).
8. L. Iommarini, A. M. Porcelli, G. Gasparre, I. Kurelac, Non-canonical mechanisms regulating hypoxia-inducible factor 1 alpha in cancer. *Front. Oncol.* **7**, 286 (2017).
9. J. P. Hoj, B. Mayro, A. M. Pendergast, A TAZ-AXL-ABL2 feed-forward signaling axis promotes lung adenocarcinoma brain metastasis. *Cell Rep.* **29**, 3421–3434.e3428 (2019).
10. S. Kharbanda *et al.*, Activation of the c-Abl tyrosine kinase in the stress response to DNA-damaging agents. *Nature* **376**, 785–788 (1995).
11. X. Sun *et al.*, Activation of the cytoplasmic c-Abl tyrosine kinase by reactive oxygen species. *J. Biol. Chem.* **275**, 17237–17240 (2000).
12. E. K. Greuber, P. Smith-Pearson, J. Wang, A. M. Pendergast, Role of ABL family kinases in cancer: From leukaemia to solid tumours. *Nat. Rev. Cancer* **13**, 559–571 (2013).
13. J. P. Hoj, B. Mayro, A. M. Pendergast, The ABL2 kinase regulates an HSF1-dependent transcriptional program required for lung adenocarcinoma brain metastasis. *Proc. Natl. Acad. Sci. U.S.A.* **117**, 33486–33495 (2020).
14. J. J. Gu *et al.*, Inactivation of ABL kinases suppresses non-small cell lung cancer metastasis. *JCI Insight* **1**, e89647 (2016).
15. Y. Matsumoto *et al.*, Reciprocal stabilization of ABL and TAZ regulates osteoblastogenesis through transcription factor RUNX2. *J. Clin. Invest.* **126**, 4482–4496 (2016).
16. J. Wang, C. Rouse, J. S. Jasper, A. M. Pendergast, ABL kinases promote breast cancer osteolytic metastasis by modulating tumor-bone interactions through TAZ and STAT5 signaling. *Sci Signal* **9**, ra12 (2016).
17. J. Colicelli, ABL tyrosine kinases: Evolution of function, regulation, and specificity. *Sci. Signal* **3**, re6 (2010).
18. D. Barila, G. Superti-Furga, An intramolecular SH3-domain interaction regulates c-Abl activity. *Nat. Genet* **18**, 280–282 (1998).
19. M. A. Cavadas *et al.*, REST mediates resolution of HIF-dependent gene expression in prolonged hypoxia. *Sci. Rep.* **5**, 17851 (2015).
20. Z. Chen, J. Sui, F. Zhang, C. Zhang, Cullin family proteins and tumorigenesis: Genetic association and molecular mechanisms. *J. Cancer* **6**, 233–242 (2015).
21. S. Bienroth, E. Wahle, C. Suter-Crazzolara, W. Keller, Purification of the cleavage and polyadenylation factor involved in the 3′-processing of messenger RNA precursors. *J. Biol. Chem.* **266**, 19768–19776 (1991).
22. C. R. Mandel, Y. Bai, L. Tong, Protein factors in pre-mRNA 3′-end processing. *Cell Mol. Life Sci.* **65**, 1099–1122 (2008).
23. Y. Sun *et al.*, Molecular basis for the recognition of the human AAUAAA polyadenylation signal. *Proc. Natl. Acad. Sci. U.S.A.* **115**, E1419–E1428 (2018).
24. S. Menon, T. Tsuge, N. Dohmae, K. Takio, N. Wei, Association of SAP130/SF3b-3 with Cullin-RING ubiquitin ligase complexes and its regulation by the COP9 signalosome. *BMC Biochem.* **9**, 1 (2008).
25. R. Oughtred *et al.*, The BioGRID database: A comprehensive biomedical resource of curated protein, genetic, and chemical interactions. *Protein Sci.* **30**, 187–200 (2021).
26. J. I. Perez-Perri *et al.*, The TIP60 complex is a conserved coactivator of HIF1A. *Cell Rep.* **16**, 37–47 (2016).
27. S. Jackson, Y. Xiong, CRL4s: The CUL4-RING E3 ubiquitin ligases. *Trends Biochem. Sci.* **34**, 562–570 (2009).
28. H. Liu *et al.*, Inflammation-dependent overexpression of c-Myc enhances CRL4(DCAF4) E3 ligase activity and promotes ubiquitination of ST7 in colitis-associated cancer. *J. Pathol.* **248**, 464–475 (2019).
29. J. B. Heidelberger *et al.*, Proteomic profiling of VCP substrates links VCP to K6-linked ubiquitylation and c-Myc function. *EMBO Rep.* **19**, e44754 (2018).
30. A. Baluapuri, E. Wolf, M. Eilers, Target gene-independent functions of MYC oncoproteins. *Nat. Rev. Mol. Cell Biol.* **21**, 255–267 (2020).
31. J. Y. Wang, The capable ABL: What is its biological function? *Mol. Cell Biol.* **34**, 1188–1197 (2014).
32. A. Khatri *et al.*, ABL kinase inhibition promotes lung regeneration through expansion of an SCGB1A1+ SPC+ cell population following bacterial pneumonia. *Proc. Natl. Acad. Sci. U.S.A.* **116**, 1603–1612 (2019).
33. Y. Xi *et al.*, Local lung hypoxia determines epithelial fate decisions during alveolar regeneration. *Nat. Cell Biol.* **19**, 904–914 (2017).
34. R. Y. Ebright *et al.*, HIF1A signaling selectively supports proliferation of breast cancer in the brain. *Nat. Commun.* **11**, 6311 (2020).
35. Y. Kim *et al.*, Methylation-dependent regulation of HIF-1alpha stability restricts retinal and tumour angiogenesis. *Nat. Commun.* **7**, 10347 (2016).
36. B. Mohapatra *et al.*, Protein tyrosine kinase regulation by ubiquitination: Critical roles of Cbl-family ubiquitin ligases. *Biochim. Biophys. Acta* **1833**, 122–139 (2013).
37. L. K. Nguyen, W. Kolch, B. N. Kholodenko, When ubiquitination meets phosphorylation: A systems biology perspective of EGFR/MAPK signalling. *Cell Commun. Signal* **11**, 52 (2013).
38. T. Hunter, The age of crosstalk: Phosphorylation, ubiquitination, and beyond. *Mol. Cell* **28**, 730–738 (2007).
39. Y. Chen *et al.*, Phosphorylation regulates cullin-based ubiquitination in tumorigenesis. *Acta Pharm Sin B* **11**, 309–321 (2021).
40. B. Tanos, A. M. Pendergast, Abl tyrosine kinase regulates endocytosis of the epidermal growth factor receptor. *J. Biol. Chem.* **281**, 32714–32723 (2006).
41. M. K. Skinner, A. Rawls, J. Wilson-Rawls, E. H. Roalson, Basic helix-loop-helix transcription factor gene family phylogenetics and nomenclature. *Differentiation* **80**, 1–8 (2010).
42. M. Mayerhofer, P. Valent, W. R. Sperr, J. D. Griffin, C. Sillaber, BCR/ABL induces expression of vascular endothelial growth factor and its transcriptional activator, hypoxia inducible factor-1alpha, through a pathway involving phosphoinositide 3-kinase and the mammalian target of rapamycin. *Blood* **100**, 3767–3775 (2002).
43. M. T. Gomez-Casares *et al.*, C-myc expression in cell lines derived from chronic myeloid leukemia. *Haematologica* **89**, 241–243 (2004).
44. K. H. Lin *et al.*, Using antagonistic pleiotropy to design a chemotherapy-induced evolutionary trap to target drug resistance in cancer. *Nat. Genet* **52**, 408–417 (2020).
45. O. Shalem *et al.*, Genome-scale CRISPR-Cas9 knockout screening in human cells. *Science* **343**, 84–87 (2014).
46. C. Cerda-Smith, Rescue of HIF1A protein level by E3-ligase KO. Gene Expression Omnibus. https://www.ncbi.nlm.nih.gov/geo/query/acc.cgi?acc=GSE228311. Deposited 27 March 2023.